NIPPON STEEL TECHNICAL REPORT No. 89 January 2004

UDC 531 . 717 . 2 : 681 . 3 : 621 . 771 . 23 . 016 . 2

Consistent Shape Prediction Simulator after Hot Rolling Mill

Harutoshi OGAI*1,*2 Masahiro ITO*1
Ryu HIRAYAMA*1

Abstract

This paper presents an outline relating to a run out table, down coiler, coil yard consistent shape prediction simulator. First, the developing motive of this simulator is described. Second, the object process, fundamental equation and model of this simulator are introduced. Following these, the configuration of this consistency shape prediction simulator and the verification by field experiment are reported.

1. Introduction

The Japanese steel industry has concentrated efforts to further reduce production costs and to enhance product quality in order to strengthen its competitive position in international markets. From the viewpoint of instrumentation and process control, however, it is felt that there are certain limitations to the cost reduction and quality enhancement by optimizing the conditions (equipment and operation conditions) of individual production processes. In this situation, efforts should be oriented toward optimization of process conditions encompassing plural sequential processes, or multi-process control, in order to realize cost reduction and quality enhancement hitherto unattained. This paper presents an outline of a newly developed technology for predicting the cold shape of a hot-rolled steel strip, named "Consistent Shape Prediction Simulator" covering a run out table, down coilers and a coil yard, as examples of positive efforts toward the multi-process control. It also discusses the results of verification through tests.

Initially, the background of the development of the shape prediction simulator is explained.

The shape control technologies of a hot-rolled steel strip began with the crown control, or profile control. Hot rolling mills of high crown/shape control capacities such as a 6-high mill and a cross roll mill were developed, and highly accurate shape/crown control was realized by adequately setting and dynamically controlling the positioning of the intermediate rolls of a 6-high mill or the cross angle of a cross roll mill and the amount of roll bending. As a result, as far as the strip shape and crown at the exit from the final rolling stand are concerned, they have come to be accurately controlled to respective target levels[1]. However, even if a hot-rolled strip has a desired shape at the exit from the final rolling mill stand, its shape changes during cooling on a run out table, coiling on a down coiler and cooling thereafter. For this reason, a desired flatness has not been realized in terms of the final strip shape in cold. Thus, to control the cold shape of a hot-rolled strip to a desired level, investigations were made on commercially produced steel strips to examine the interrelation between the strip shape immediately after the finish hot rolling and that after being cooled. Despite all these, a shape control model capable of realizing a desired cold shape was not worked out.

In consideration of the above, the authors entered upon developing a simulator to predict the shape of a hot-rolled strip after cooling using physical models. There had been a report of an analysis of the shape of a strip after cooling on a run out table[8], but a shape prediction covering the steps of coiling on a down coiler, deformation while in the form of a coil and uncoiling in cold had not been brought to practical reality.

2. Object Process

A steel slab is rolled into a strip of a prescribed thickness through the finishing mill stands of a hot rolling mill, the strip is cooled by the cooling equipment of a run out table (ROT) at a cooling rate and a cooling pattern prescribed according to steel grade and thickness and then, it is wound into a coil on a down coiler (DC). The strip shape immediately after the finish rolling is measured with a shape meter provided at the exit from the final mill stand. In addition, radiation thermometers are established at the exit from the final mill stand and the ROT to measure strip temperature at its width center and the temperature distribution in the width direction.

After coiling, a coil is transported to a coil yard (cooling bed) and cooled with air or water to room temperature.

A coil cooled to room temperature is uncoiled on a finishing and conditioning line for inspection and leveling. The cold shape of a

*1 Environment and Process Research Center

*2 Waseda University (Graduate School of Information, Production and Systems)

hot-rolled strip mentioned earlier is the shape that becomes apparent at this stage.

3. Concept and Fundamental Equations of Shape Prediction Simulator

The developed shape prediction simulator deals with a phenomenon in which the thermal conduction, structural transformation and stress-strain behaviors that occur in a steel strip at an ROT, a DC and a coil yard are entwined with each other as shown in **Fig. 1**.

It predicts the shape of a steel strip that becomes apparent upon its uncoiling at the finishing and conditioning stage by calculating the changes of stress and strain of an object strip at cross sections (C sections) normal to the rolling direction at several longitudinal positions (top, middle and bottom, for example). The changes of stress and strain result from the cooling applied during the course after the finish hot rolling to the product finishing and conditioning, the transformations during the course and the work of the coiling and uncoiling. The simulator calculates the stress and strain changes in a consistent manner covering the steps of the ROT, DC and coil yard.

The simulation is done by passing on the information of the distributions of temperature, transformation ratio, stress and strain at a C section of an object strip at a process step to a subsequent process step as shown in **Fig. 2**. Here, regarding the cooling after the finish hot rolling, the heat generated by exothermic transformation must be taken into consideration. In addition, it is necessary to calculate the stress-strain distribution using Young's modulus and a linear expansion coefficient. Furthermore, in both of these the calculated distributions of temperature and transformation ratio have to be taken into account. It is also necessary at a DC to take into account the influence of coiling tension over the stress-strain distribution and, at a finishing and conditioning line, the shape that becomes apparent upon uncoiling.

The simulator calculates the temperature, transformation, stress and strain at a C sections of a steel strip and, based on the results of these items, calculates the shape of the strip.

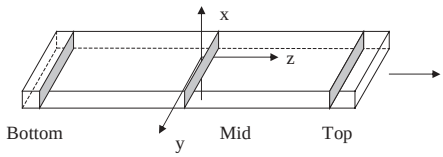

Fig. 3 Coordinate system (C section) of shape prediction simulator

The fundamental equations used in the developed shape simulator at different production process steps are explained hereafter.

Symbols

T: steel temperature [K], t: time [s], ρ: density [kg/m^3], c: specific heat [J/kg·K], λ: thermal conductivity [W/m^2·K], q: transformation heat generation [W], x: coordinate in the thickness direction, y: coordinate in the width direction, ε_x: strain in the x direction, σ_x: stress in the x direction [N/m^2], E: Young's modulus [N/m^2], ε_x^p: plastic strain in the x direction, ε_T: expansion coefficient, ν: Poisson ratio, τ_{xy}: sectional shear force at an x-y plane [N/m^2].

Note that the specific heat c does not include magnetism latent heat, and that the meaning of a symbol with a suffix is fundamentally the same if the suffix is changed.

Fig. 3 shows the coordinate system of a C section of a steel strip.

3.1 Run out table (ROT)

3.1.1 Heat transfer model

Here, a 2-dimensional non-steady model within a C section is considered. Thermal conductivity is given as a function of strip temperature.

Fundamental equation: $$\frac{\partial T}{\partial t} = \frac{1}{\rho c}\left\{\frac{\partial}{\partial x}\left(\lambda\frac{\partial T}{\partial x}\right) + \frac{\partial}{\partial y}\left(\lambda\frac{\partial T}{\partial y}\right)\right\} + \frac{q}{\rho c} \quad (1)$$

Boundary condition: $$\lambda\frac{\partial T}{\partial t} = h(T - T_w) \quad (2)$$

A ROT cooling model sets the value of thermal conductivity h in the

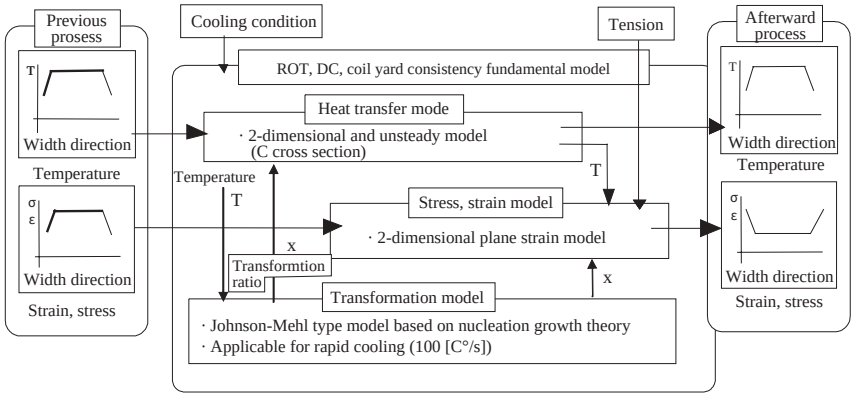

Fig. 1 Synthetic model combining heat transfer model, transformation model and stress-strain model

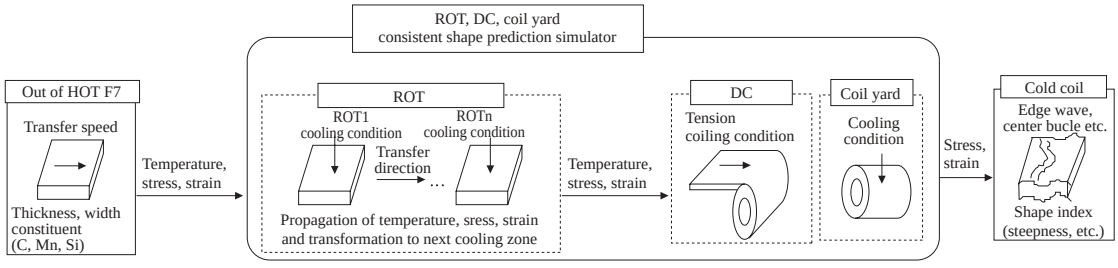

Fig. 2 Consistent shape prediction simulator for hot-rolled steel strip

Table 1 Johnson-Mehl type transformation models

Transformation	Transformation speed	Nucleation and growth rate	Coefficient
Ferrite	Nucleation-growth $\frac{dx}{dt} = 4.046\left(k_1\frac{6}{d_\gamma^4}\tau IG^3\right)^{1/4}\left(\ln\frac{1}{1-x}\right)^{3/4}(1-x)$	$1 = T^{-1/2}D \cdot \exp\left(-\frac{k_3}{RT\Delta G_V^2}\right)$ $G = \frac{1}{2r}D\frac{C_{\gamma\alpha}-C_\gamma}{C_\gamma-C_\alpha}$	$k_1 = 1.7476 \cdot 10^6$ $k_2 = 8.933 \cdot 10^{-12}\exp\left(\frac{21100}{T}\right)$ $k_3 = \left(cal^3/mol^3\right) = 0.957 \cdot 10^9$
Pearlite	Saturation-growth $\frac{dx}{dt} = k_2\frac{6}{d_\gamma}G(1-x)$	$G = \Delta T \cdot D \cdot \left(C_{\gamma\alpha}-C_{\gamma\beta}\right)$	$k_2 = 6.72 \cdot 10^6$
Bainite		$G = \frac{1}{2r}D \cdot \frac{C_{\gamma\alpha}-C_\gamma}{C_\gamma-C_\alpha}$	$k_2 = 6.816 \cdot 10^{-4}\exp\left(\frac{3431.5}{T}\right)$

d_γ: γ particle size, D[m]: diffusion coefficient of C in γ [m²/s], C_γ: C mole fraction concentration in γ, C_α : C mole fraction concentration in ferrite, $C_{\gamma\alpha}$: C molarity in γ of the γ /α interface, $C_{\gamma\beta}$: C molarity in γ of the γ /cem interface, ΔT: super cooling from Ae_1 [K], r: curvature radius of a growth interface

boundary condition of Equation (2) for either water cooling or air cooling depending on the cooling condition of an ROT. In the case of water cooling, an equation for spray cooling is used[6].

$h = W^\alpha + \beta$, $\alpha = 0.8$, $\beta = 100$

3.1.2 Exothermic transformation model

Johnson-Mehl type models based on the nucleation growth theory are used as the transformation progress models of the developed simulator[7].

The transformation progress models shown in **Table 1** are used for calculating the distribution of transformation ratio X in a C section at a prescribed position of a steel strip. A ferritic transformation ratio XF, a pearlitic transformation ratio XP and a bainitic transformation ratio XB are calculated, respectively, by transformation progress models of ferritic, pearlitic and bainitic transformations. A sum of these transformation ratios is used as the transformation ratio X of a steel strip.

The transformation ratio X thus obtained is used for calculating the transformation heat generation q per unit volume and unit time.

$$q = \rho\left[q_1\frac{\partial X}{\partial t} + \frac{\partial}{\partial t}(q_m \cdot X)\right] \quad (3)$$

$$q_m = \int (c_\alpha - c)dT \quad (3')$$

The transformation heat generation q above is calculated as a sum of the latent heat q_l [J/kg] resulting from lattice transformation and the magnetism latent heat q_m [J/kg] resulting from the change of magnetism as seen in Equation (3). The magnetism latent heat q_m is calculated using Equation (3') from the actual measurement of specific heat.

3.1.3 Stress-strain model

Stress and strain are calculated using a 2-dimensional plane strain model regarding a C section of a steel strip under the following assumptions.

Assumption 1: homogeneity in the z direction.

Assumption 2: body force = 0.

Assumption 3: $\tau_{xz} = 0$, $\tau_{yz} = 0$.

· The relational expressions of stress and strain are as follows:

$$\varepsilon_x = \frac{1}{E}\{\sigma_x - \nu(\sigma_y + \sigma_z)\} + e_x,\ e_x = \varepsilon_x^p + \varepsilon^T$$
$$\varepsilon_y = \frac{1}{E}\{\sigma_y - \nu(\sigma_z + \sigma_x)\} + e_y,\ e_y = \varepsilon_y^P + \varepsilon^T$$
$$\varepsilon_z = \frac{1}{E}\{\sigma_z - \nu(\sigma_x + \sigma_y)\} + e_z,\ e_z = \varepsilon_z^P + \varepsilon^T$$
$$\gamma_{xy} = \frac{1}{G}\tau_{xy} + \gamma_{xy}^P$$
$$\gamma_{yz} = \frac{1}{G}\tau_{yz} = 0$$
$$\gamma_{zx} = \frac{1}{G}\tau_{zx} = 0$$
$$G = \frac{E}{2(1+\nu)} \quad (4)$$

· The balance equations of force are as follows (the derivative in the z direction is 0):

$$\frac{\partial\sigma_x}{\partial x} + \frac{\partial\tau_{xy}}{\partial y} = 0$$
$$\frac{\partial\tau_{xy}}{\partial x} + \frac{\partial\sigma_y}{\partial y} = 0 \quad (5)$$

· The compatibility condition of strain is as follows:

$$\frac{\partial^2\gamma_{xy}}{\partial x\partial y} = \frac{\partial^2\varepsilon_x}{\partial y^2} + \frac{\partial^2\varepsilon_y}{\partial x^2} \quad (6)$$
$$\varepsilon_z = const$$

Equations (7) below are obtained by transforming Equation (6) and introducing a stress function ϕ.

$$\nabla^4\varphi = -E_e[\nu\nabla^2 e_z + g],\ E_e = \frac{E}{1-\nu^2}$$
$$g = \frac{\partial^2\gamma_{xy}^{2p}}{\partial x\partial y} - \left(\frac{\partial^2 e_x}{\partial y^2} - \frac{\partial^2 e_y}{\partial x^2}\right)$$
$$\sigma_x = \frac{\partial^2\varphi}{\partial y^2}$$
$$\sigma_y = \frac{\partial^2\varphi}{\partial x^2} \quad (7)$$
$$\tau_{xy} = -\frac{\partial^2\varphi}{\partial x\partial y}$$

Boundary condition: free boundary $\frac{\partial\varphi}{\partial y} = 0$, $\frac{\partial\varphi}{\partial x} = 0$

$$\sigma_P^2 = \sigma_x^2 + \sigma_y^2 + \sigma_z^2 - \sigma_x\sigma_y - \sigma_y\sigma_z - \sigma_z\sigma_x + 3\tau^2$$

· Yield condition: $P = \sigma_P^2 - Y^2 = 0$ (8)

· Plastic strain increments are as follows:

$$\Delta\varepsilon_x^P = \lambda'\frac{\partial P}{\partial\sigma_x} = \lambda\{\sigma_x - (\sigma_y + \sigma_z)/2\}$$
$$\Delta\varepsilon_y^P = \lambda'\frac{\partial P}{\partial\sigma_y} = \lambda\{\sigma_y - (\sigma_z + \sigma_x)/2\}$$
$$\Delta\varepsilon_z^P = \lambda'\frac{\partial P}{\partial\sigma_z} = \lambda\{\sigma_z - (\sigma_x + \sigma_y)/2\} \quad (9)$$
$$\Delta\gamma_{xy}^P = 3\lambda\tau_{xy}$$

Stress and strain are calculated by the convergence method, wherein the value of λ is searched and corrected, as shown in **Fig. 4**. Models taking into consideration the temperature and transforma-

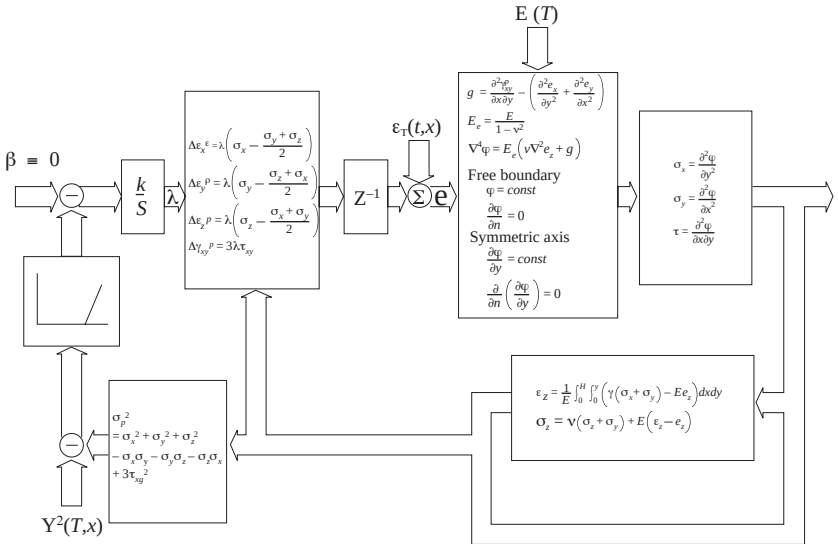

Fig. 4 Stress-strain calculation through search of λ value

tion ratio of a steel strip are used for the Young's modulus and the coefficient of linear expansion.

3.2 Down coiler (DC)

At a down coiler, a steel strip is wound into a coil, and it is dealt with as a cylindrical object in which positions along the strip length (L direction) correspond to the positions of laminated and nearly-concentric layers as shown in **Fig. 5**. Here, a C section at a prescribed position of a steel strip is located at the inner-most lap, at any one of the middle laps, or at the outer-most lap of a coil. That is to say, a C section at the top of a strip is positioned at the inner-most lap of a coil and, as the position of the C section goes away from the strip top, its position in a coil moves to the middle and, finally, to the outer-most lap.

3.2.1 Heat transfer model

The boundary condition of thermal conductivity at a C section is determined depending on which portion of a coil the C section in question is in. At a C section in the outer-most or innermost lap of a coil, a convective heat transfer coefficient (air cooling condition) is set for the sides directly contacting the atmosphere, namely the outer-most or innermost coil surface and the strip edges, and an ordinary heat transfer coefficient (a constant) for a side contacting an adjacent lap. At a C section in a middle lap of a coil, a convective heat transfer coefficient (air cooling condition) is set for strip edges only. The temperature distribution history of a C section at a prescribed position of a strip is calculated using the heat transfer model of Equation (1).

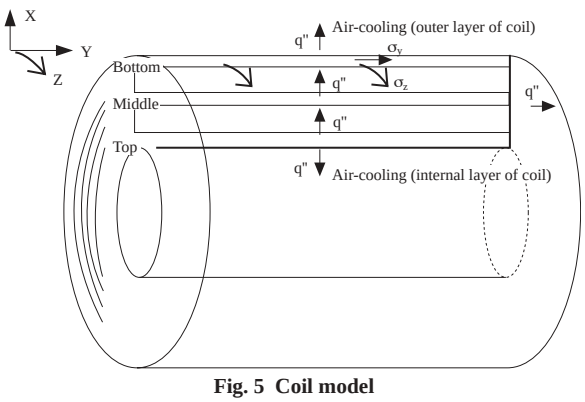

Fig. 5 Coil model

3.2.2 Stress-strain model

This model calculates the stress distribution in a C section at a prescribed position of a strip in coil.

3.3 Coil yard and uncoiling

3.3.1 Heat transfer model

The boundary conditions are set in the same manner as those of the cooling conditions at a down coiler.

3.3.2 Stress-strain model

This model calculates the stress and strain at the uncoiling after a steel strip in coil is cooled to room temperature.

3.4 Cold shape prediction model

This model calculates shape indices $\Lambda_1 - \Lambda_4$ from the stress and strain after the uncoiling, which are calculated using the stress-strain model above.

Strain difference $\Delta\varepsilon_i$ between each of longitudinal strip elements (fibers), which are supposedly arranged abreast in the width direction, and the width center is calculated from the thickness direction average of longitudinal stress as shown in Equation (10).

$$\Delta\varepsilon_i = \left(\frac{\bar{\sigma}_i}{E(\bar{T}_i)} - \frac{\bar{\sigma}_o}{E(\bar{T}_o)}\right) \tag{10}$$

Next, the width direction pattern of the strain differences of the strip elements is approximated by the least square method using the quartic function of Equation (11).

$$f(y) = \lambda_0 + \lambda_1 \cdot y + \lambda_2 \cdot y^2 + \lambda_3 \cdot y^3 + \lambda_4 \cdot y^4 \tag{11}$$

Then, the shape indices $\Lambda_1 - \Lambda_4$ are calculated through linear transformation of $\lambda_1 - \lambda_4$ as shown in Equation (12).

$$\begin{bmatrix}\Lambda_1\\ \Lambda_2\\ \Lambda_3\\ \Lambda_4\end{bmatrix} = \begin{bmatrix} 1 & 0 & 1 & 0\\ 0 & 1 & 0 & 1\\ 1/\sqrt{3} & 0 & 1/3\sqrt{3} & 0\\ 0 & 1/2 & 0 & 1/4\end{bmatrix}\begin{bmatrix}\lambda_1\\ \lambda_2\\ \lambda_3\\ \lambda_4\end{bmatrix} \tag{12}$$

Among the shape indices $\Lambda_1 - \Lambda_4$ thus obtained, the indices Λ_1 and Λ_3 represent asymmetric components in the width direction and the indices Λ_2 and Λ_4 symmetric components. Here, among the symmetric components in the quartic function approximation of the strip shape, the index Λ_2 shows the strain difference between the width

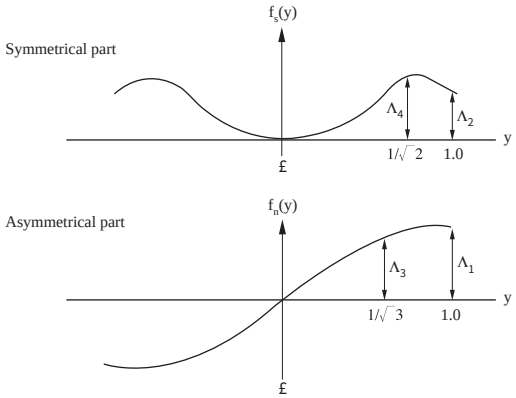

Fig. 6 Shape indices (Λ_2, Λ_4 and Λ_1, Λ_3)

center and both the edges, and the index Λ_4 that between the width center and the position of $1/\sqrt{2} \times 1/2 \times$ B from the center, where B is the strip width (see **Fig. 6**).

4. Shape Prediction Simulator for Hot-rolled Steel Strip

4.1 Structure of shape prediction simulator

The shape prediction simulator, which incorporates the heat transfer models, transformation progress models, stress-strain models and shape prediction model explained in the previous section, is constructed on a simulator building environment called TRAS[5] developed by Nippon Steel. **Fig. 7** shows a module to calculate the conditions of temperature, transformation and stress at one of the cooling zones of an ROT.

Since an ROT is usually divided into several cooling zones, some water-cooling zones and some air-cooling zones, a calculation module is provided for each of these zones, and calculations are done in accordance with the conditions of each zone. In the example shown in **Fig. 8**, there are 5 cooling zones. The calculations regarding a prescribed strip section is completed by passing the information of temperature, transformation ratio and stress calculated by a module at one zone on to the module of the following zone downstream.

Fig. 9 shows the calculation modules of a down coiler; here one module is allocated for each of the 3 portions of a coil, or the top, middle and bottom.

The developed simulator can calculate the strip shape, covering consistently from an ROT through a DC and a coil yard to the uncoiling on a finishing and conditioning line, by sequentially linking calculation modules. The simulator carries out the calculations in synchronization with the tracking of several strip sections along its length and thanks to this, the shapes at different longitudinal positions of a strip can be calculated; this enables dynamic shape control and simulation. Since the modules of the developed simulator calculate at a high speed by the finite difference method, real-time application is viable.

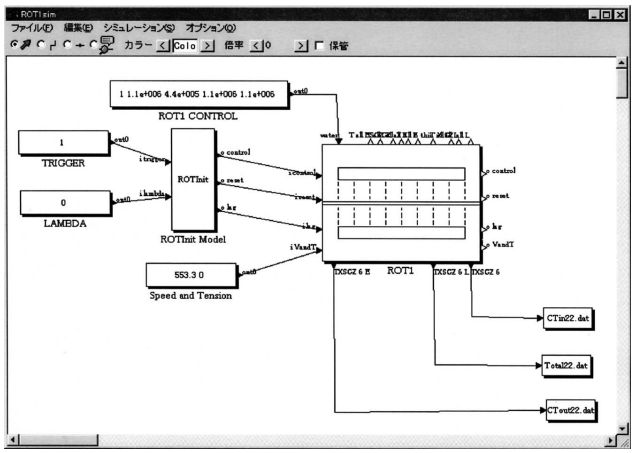

Fig. 7 Basic module of one cooling zone

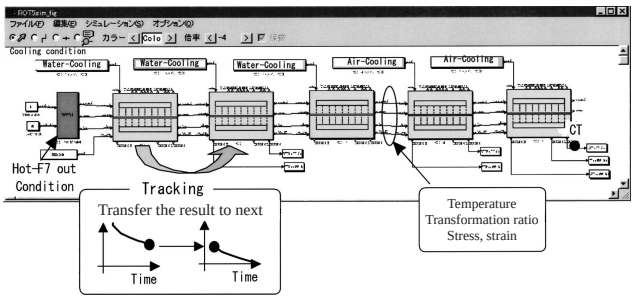

Fig. 8 Simulator of ROT composed of 5 cooling zones

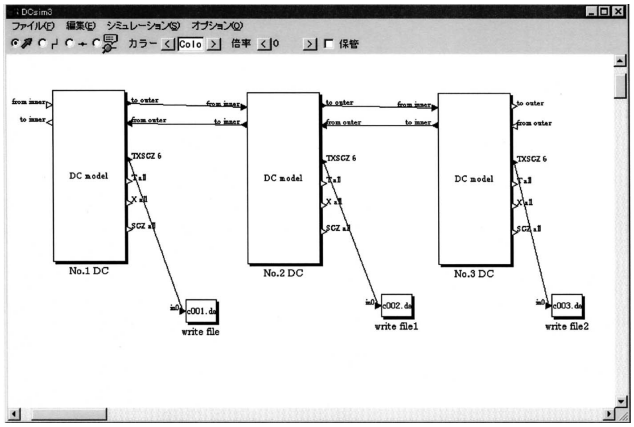

Fig. 9 Simulator modules for one DC

4.2 Verification

The calculation results regarding a cooling zone of a run out table obtained by the developed simulator were compared with those obtained by the finite element method (MARC). As seen in **Fig. 10**, the results of the developed simulator (TRAS) were nearly the same as those of MARC.

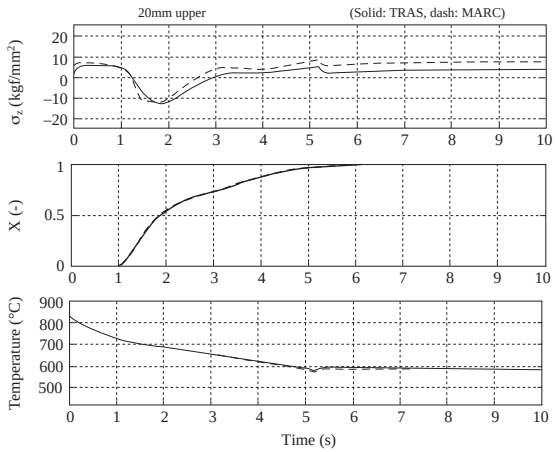

Fig. 10 Verification of simulation accuracy at one cooling zone

5. Study of Shape Change Mechanisms and Verification through Field Tests

5.1 Test conditions and measurement items

A test of consistent measurements of strip temperature and shape was carried out at one of Nippon Steel's hot strip mills, covering from the ROT to the finishing and conditioning line. Because there had been very few cases of sequentially tracking the temperature and shape histories of a hot-rolled strip, the test yielded precious data. The test conditions and the measured items are shown in **Fig. 11**.

5.2 Evaluation of calculation results

5.2.1 Calculation results for ROT, DC and coil yard

Calculation results of the developed simulator at an ROT and from a DC to a coil yard are shown in **Fig. 12**. Temperature data were used for adjusting the thermal conductivity in the heat transfer models of the simulator, and by this the calculation results were made to agree with measurement results as seen in the figure.

Fig. 13 shows an example of multi-process calculation of residual stress change at the top of a strip from an ROT to uncoiling at room temperature. It is possible to understand from the figure the mechanism of strip shape change from an ROT through a DC and a coil yard to a finishing and conditioning line. There was tension at both the strip edges (center waviness) during cooling at the ROT, but the tension at the edges was mitigated during coiling at the DC, and as a result center waves disappeared and edge waves appeared. The edge waviness was increased during cooling at the coil yard, and then, at the uncoiling on the finishing and conditioning line after cooling to room temperature, the edge waviness was partially mitigated, but it still remained in the final sheet products.

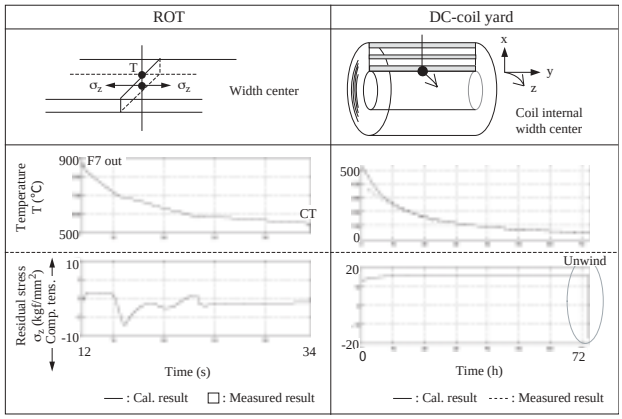

Fig. 12 Example calculation for ROT, DC and coil yard

5.2.2 Verification of shape prediction model

The cold shape predicting accuracy of the developed simulator was evaluated through comparison with the results of actual measurement on a finishing and conditioning line.

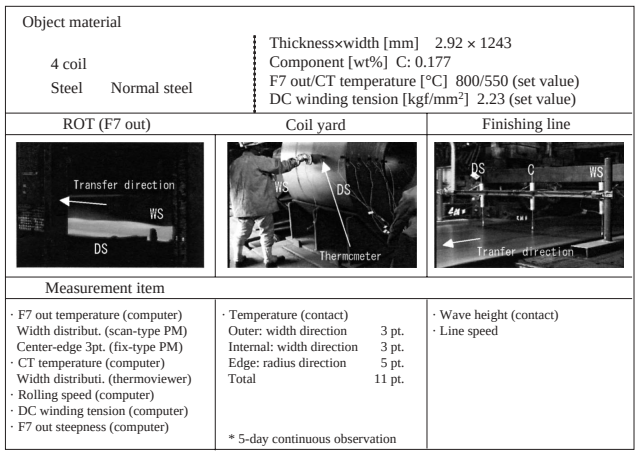

Fig. 11 Test conditions and measurement items

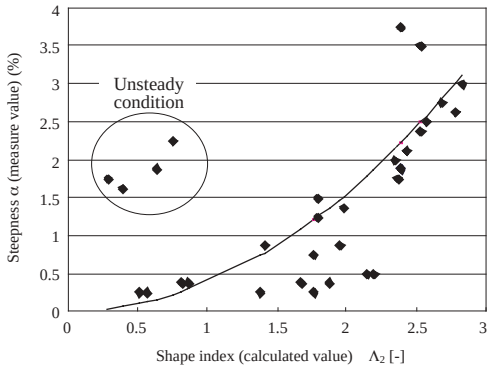

Fig. 14 Predictions and measurements of final product shapes

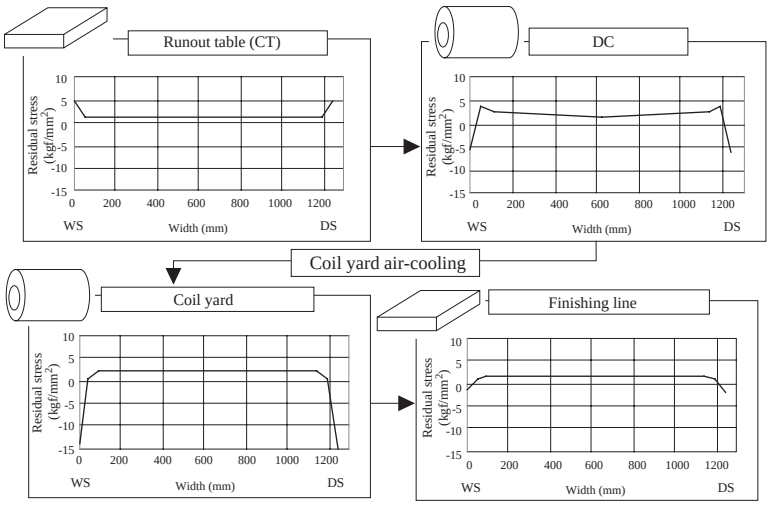

Fig. 13 Example calculation of residual stress change (from ROT to finishing line, strip top portion)

Fig. 14 shows the comparison of the strip shapes predicted by the simulator and those actually measured. The actually measured shapes are plotted in terms of steepness and the calculated shapes in terms of a shape index corresponding to elongation and, hence, they are in a quadratic relation. Most of the calculated shapes agreed well with the measured shapes. Some data in which the two did not agree represented unsteady strip portions, and they should have been omitted from the comparison. The above comparison made it clear that the developed simulator was capable of consistent (multi-process) shape prediction.

6. Summary

A consistent shape prediction simulator for a hot-rolled steel strip covering a run out table, down coilers and a coil yard was developed. The calculation models and modules of the simulator and the comparison of the shape prediction results of the simulator with actual measurements have been explained in this paper. The developed simulator proved to be capable of consistently predicting the shape of a hot-rolled steel strip.

The simulator is slated for application to actual commercial production for the purpose of predicting the strip shape at a finishing and conditioning line. The authors intend to further examine the shape prediction results of the simulator product by product and based on the examination, establish a technology to automatically realize a target shape of a hot-rolled steel strip. Furthermore, the concept of the developed simulator is expected to open the possibility of other new control technologies covering multiple process steps.

References

1) Naganuma, Y., Takahashi, H., Ogai, H., Baba, K., Masuda, S.: Seitetsu Kenkyu. (317), 41(1985)
2) Naganuma,Y.,Takahashi,H., Ogai,H.:Nippon Steel Technical Report,(27),43(1985)
3) Naganuma,Y.,Ogai,H.: Control-Theory and Advanced Technology.1-1, 47 (1985)
4) Naganuma,Y.,Takahashi,H.,Ogai,H.: Preprint of IFAC Automation in Mining,Mineral and Metal Processing. 354 (1986)
5) Konno, Y., Shioya, M, Ueyama, T.: Shinnittetsu Giho. (257), 53(1995)
6) Mitsuzuka, M., Fukuda, K.: Tetsu-to-Hagané. 69(1983)
7) Yada, Senuma: J. of Japan Institute of Metals. 29(6), 430(1990)
8) Yoshida, Sasaki, Tanaka, Hirose: Tetsu-to-Hagané. 68(8), 71(1982)
9) Ogai,H.,Ito,M.,Hirayama,R.:Preprint of IFAC Automation in Mining,Mineral and Metal Processing. 63 (2001)
10) Ogai, H., Ito, M., Hirayama, R.: Metals Industry Committee, Inst. Elec. Engrs. of Japan. 0MID-02-7, 29 (2002)
11) Ogai, H., Ito, M., Hirayama, R.: Proc. Electronics & Information System Division Conference, Inst, Elec. Engrs. of Japan. 692 (2002)